Ultrasonics - Sonochemistry 61 (2020) 104826

Contents lists available at ScienceDirect

Ultrasonics - Sonochemistry

journal homepage: www.elsevier.com/locate/ultson

Liposome destruction by hydrodynamic cavitation in comparison to chemical, physical and mechanical treatments

Žiga Pandur[a,b], Iztok Dogsa[a], Matevž Dular[b], David Stopar[a,*]

[a] University of Ljubljana, Biotechnical Faculty, Večna pot 111, Ljubljana 1000, Slovenia
[b] University of Ljubljana, Faculty of Mechanical Engineering, Aškerčeva 6, Ljubljana 1000, Slovenia

ARTICLE INFO

Keywords:
Hydrodynamic cavitation
Giant lipid vesicles
DOPC
Stability
Fluorescein release
Confocal laser microscopy

ABSTRACT

Liposomes are widely applied in research, diagnostics, medicine and in industry. In this study we show for the first time the effect of hydrodynamic cavitation on liposome stability and compare it to the effect of well described chemical, physical and mechanical treatments. Fluorescein loaded giant 1,2-dioleoyl-*sn*-glycero-3-phosphocholine (DOPC) lipid vesicles were treated with hydrodynamic cavitation as promising method in inactivation of biological samples. Hydrodynamic treatment was compared to various chemical, physical and mechanical stressors such as ionic strength and osmolarity agents (glucose, Na^+, Ca^{2+}, and Fe^{3+}), free radicals, shear stresses (pipetting, vortex mixing, rotational shear stress), high pressure, electroporation, centrifugation, surface active agents (Triton X-100, ethanol), microwave irradiation, heating, freezing-thawing, ultrasound (ultrasonic bath, sonotrode). The fluorescence intensity of individual fluorescein loaded lipid vesicles was measured with confocal laser microscopy. The distribution of lipid vesicle size, vesicle fluorescence intensity, and the number of fluorescein loaded vesicles was determined before and after treatment with different stressors. The different environmental stressors were ranked in order of their relative effect on liposome fluorescein release. Of all tested chemical, physical and mechanical treatments for stability of lipid vesicles, the most detrimental effect on vesicles stability had hydrodynamic cavitation, vortex mixing with glass beads and ultrasound. Here we showed, for the first time that hydrodynamic cavitation was among the most effective physico-chemical treatments in destroying lipid vesicles. This work provides a benchmark for lipid vesicle robustness to a variety of different physico-chemical and mechanical parameters important in lipid vesicle preparation and application.

1. Introduction

A liposome or lipid vesicle is a lipid bilayer rolled up into a spherical shell with enclosed liquid within shell, which is separated from the outer (surrounding) liquid solution. Because of this fundamental similarity to the biological cell membrane, lipid vesicles have been used extensively as model systems to study properties and stability of lipid bilayers to different physico-chemical or biochemical parameters [1–5]. Lipid bilayer integrity is one of the main criteria to distinguish between viable and dead cells. If cell membrane is compromised, the essential cellular components leak out which results in cell death [6]. To assess bacteria viability, the membrane impermeable fluorescent dyes are regularly used (i.e. propidium iodide) [7–10]. Normally cell membranes are impermeable to a charged dye propidium iodide. However, if cell membrane is compromised, propidium iodide can enter into the cell and intercalate with DNA which increases its fluorescence quantum yield [10]. Consequently, dead cells become fluorescent and can be distinguished from live cells with intact membranes, which are impermeable to propidium iodide [9]. In this work we have reversed the logic and packed fluorescence dye fluorescein inside the lipid vesicle and measured its leakage to the surrounding media upon hydrodynamic cavitation and other different physico-chemical treatments.

There are numerous protocols to make lipid vesicles of different size, lamellarity and composition reviewed by Laouini et al. [11]. Liposomes are classified according to vesicular size and lamellar structure as small unilamellar vesicles (20–40 nm), medium (40–80 nm), large (100–1000 nm) or giant (> 1000 nm) vesicles [12]. Oligolamellar vesicles are made from 2 to 10 bilayers, whereas multilamellar vesicles have several bilayers. Intrinsically the stability of lipid vesicles is dependent on curvature elastic free energy. Using model membranes, two

Abbreviations: DOPC, 1,2-dioleoyl-*sn*-glycero-3-phosphocholine; GUV, giant unilamellar vesicles; HC, hydrodynamic cavitation; DIC, differential interference contrast microscopy

* Corresponding author.
E-mail address: david.stopar@bf.uni-lj.si (D. Stopar).

https://doi.org/10.1016/j.ultsonch.2019.104826
Received 12 June 2019; Received in revised form 9 August 2019; Accepted 8 October 2019
Available online 19 October 2019

instabilities could be observed: rupture and buckling. The former can be seen during pore formation and fragmentation, as a result of local perturbations of lipid organization [13], the latter gives rise to membrane bending or folding due to leaflet asymmetry or membrane tension modifications [14,15]. Generally, more curved the lipid vesicle, easier it is to fuse or break. This suggests that large or giant lipid vesicles should be more stable than smaller vesicles. Although the total curvature elastic free energy for a spherical liposome is the same for every size of sphere, its free energy for unit lipid is much higher for smaller vesicles. As the number of lipids in the vesicle decreases with smaller vesicles, the curvature free energy per lipid scales as R^2. This explains why supported lipid bilayers are made from unstable small vesicles rather than the other way around [16].

In spite of their great inherent stability, lipid vesicles constantly undergo remodelling, fusion, pore formation, and various means of lipid exchange [17–19]. The long-term stability of lipid vesicles can be dramatically affected by lipid acyl chain saturation. For example, saturated lipids are more resistant to oxidation than monounsaturated, which in turn are more stable compared to polyunsaturated lipids [20]. Lipid vesicles may be further destabilized by hydrolytic degradation. The lipid hydrolysis is dependent on several key factors including pH [21,22], temperature [22], buffer species [23,24], ionic strength [25,26], acyl chain length [27,28], headgroup composition [29] or state of the aggregation [30]. A major challenge to lipid vesicle stability is also mechanical stress, i.e. ultrasound [31], oscillating electric field [32,33], static pressure [34] and shock waves [35]. Due to their amphipathic nature lipid vesicles integrity can be easily compromised by the addition of surface-active molecules. Amphipathic compounds increase permeability of lipid vesicles by intercalating into lipid bilayer, which at concentrations higher than critical micellar concentrations, leads to disruption and solubilisation of lipid bilayer [36,37].

Although lipid vesicles can be destroyed in many ways, destruction of lipid vesicles with hydrodynamic cavitation (HC) has not been exploited yet. Cavitation occurs when small vapour bubbles are formed in liquid. Bubbles are triggered by sudden local decrease in pressure [38]. During pressure change, the bubble violently collapses and possibly rebounds, therefore extreme conditions near proximity of the bubble are likely to occur. It has been reported that extreme high temperatures (several 1000 K [39]) microjet formation (with fluid velocity up to 100 m/s [40]), pressure waves shocks (up to 100 MPa [41]), and formation of highly reactive radicals [42] may occur during bubble collapse. Due to its properties hydrodynamic cavitation has been used as the promising new treatment for bacterial inactivation [43–47]. The exact mechanism of bacteria inactivation, however, is still unknown [48]. The extreme conditions during collapse of the bubbles could have effect on bacterial cells, including the cell membrane. It is generally assumed that bacteria die because of membrane disruption [44,49,50]. Here, we report about the significant effect of hydrodynamic cavitation on model membrane leakage and stability.

To check the effect of hydrodynamic cavitation we have used giant lipid vesicles which are intrinsically more stable to breakage and better resist pore formation or fusion compared to smaller vesicles. We have focused the study on DOPC giant unilamellar lipid vesicles. The DOPC contains monounsaturated oleic acid (18:1, *cis*-9) and has often been used as a model lipid bilayer system [51–56]. The lumen of the vesicles was labelled with membrane impermeable fluorescent marker fluorescein. In the event of bilayer damage, the leakage of fluorescent marker is expected. We have employed a new fluorescence microscopy method to measure the fluorescence intensity of individual lipid vesicle loaded with fluorescein. The fluorescence intensity of the individual lipid vesicles was measured to determine the distribution of lipid vesicle size, shape, and dynamic response to hydrodynamic cavitation treatment and other physico-chemical stressors. Hydrodynamic cavitation was selected as a promising novel unexploited method in biological samples disruption, while other physico-chemical stressors have been selected to represent common challenges, to which lipid vesicles (phospholipid bilayers) are exposed. Results indicate high potency of hydrodynamic cavitation for lipid vesicle destruction. This work provides a benchmark for lipid vesicle sensitivity to hydrodynamic cavitation treatment and to a variety of different physico-chemical parameters.

2. Materials and methods

2.1. Preparation of giant unilamellar lipid vesicles (GUV)

Giant DOPC unilamellar lipid vesicles were prepared as described by Moscho et al. [57]. By applying rapid evaporation method, the procedure allows the formation of preferentially unilamellar giant lipid vesicle. Shortly, DOPC was dissolved in chloroform to a concentration of 0.1 M. Then 115 μL of lipid solution was transferred into 250 mL round bottom flask containing 5.6 mL chloroform and 572 μL of methanol. Next, 40 mL of buffer solution (10 mM HEPES buffer, pH = 7.4) with added fluorescein sodium salt - ThermoFisher Scientific, USA (375 mg/mL) was carefully added along the flask walls to lipid solution. Organic solvent was removed with rotary evaporator (Büchi Rotavapor R-134, Büchi Waterbath B-480, Büchi Vacuum Controller V-850, Büchi Vacuum pump V-700) at 40 rpm under reduced pressure (final pressure 55 mbar, volume flow rate 1.8 m^3/h) in a water bath with temperature set at 40 °C. Around evaporation point of chloroform and methanol we slowly reduced pressure in 5 mbar increments to obtain gentle boiling point of solution. After reaching final pressure of 55 mbar, we let solution to stay at that pressure for 2 min. In the next step, we separated vesicle fraction from the aqueous solution and excess fluorescein with centrifuging at 15700 × g for 10 min. Lipid vesicles in the pellet were resuspended in 40 mL 10 mM HEPS buffer. We repeated lipid vesicle washing three times, and after the third time vesicles were concentrated into 5 mL HEPES buffer. For all lipid vesicle stability experiments vesicles were prepared freshly. Lipid vesicle size was determined with DIC and fluorescence microscopy. As demonstrated by Moscho et al. [57] the method enables a simple, fast and effective method for the production of preferentially giant unilamellar DOPC lipid vesicles.

2.2. Stability of lipid vesicles

Giant DOPC lipid vesicles were exposed to different chemical, physical and mechanical stresses. For the stability experiments the concentration of GUV were between 10^6 and 10^7 vesicles/mL. Lipid vesicles were exposed to different stress exposure times up to 60 min. All reagents were prepared and diluted in 10 mM HEPES buffer solution. All experiments (except heating, freezing, and hydrostatic pressure) were made under ambient conditions (room temperature, ambient air pressure). The following conditions with intention to compromise GUV stability were tested:

a) Hydrodynamic cavitation: HC was obtained with circular Venturi restriction tube, which was made from acrylic plastic with restriction hole diameter of 0.6 mm (technical drawing of venturi restriction is represented in Supplementary Fig. S21). 5 mL of sample was pushed through Venturi restriction from one syringe to another in 0.3 s, leading to the average velocity in the order of 50 m/s inside the Venturi. Despite the limitations, which were raised by Šarc et al. [58], we still estimated the value of cavitation number, which may be useful for reference and guidance, especially in the case of upscaling. Considering the downstream pressure, the vapor pressure at 22 °C and the flow velocity inside the restriction tube, the cavitation number of $\sigma = 0.93$ can be determined. This is close, but still above the limit of chocked flow, which occurs at $\sigma = 0.045$. We pushed sample though restriction 100 times.
b) Ultrasonic treatment: 800 μL of GUV solution was put into 1.5 mL microtubes and sonicated with ultrasonic horn probe type (MSE 150 W Ultrasonic disintegrator Mk2, exponential probe 1/8″ –

3 mm) at nominal frequency of 20 kHz and at different amplitudes (3 μm, 6 μm, 9 μm, 12 μm, 15 μm, 18 μm, 21 μm) for 5 s. Horn was immersed into solution approximately 1/3 of whole sample volume. Samples were kept in cold ice water.

c) Solubilization of lipid vesicles with Triton X-100: 9 μL of fluorescein loaded GUV solution was put on microscope slide and mixed with 1 μL of appropriate Triton X-100 solution (final concentrations of Triton X-100: 0.03, 0.05, 0.11, 0.21, 0.43, 0.85, and 1.7 mM). Samples were incubated at room temperature for up to 10 min.

d) Changing osmolarity of the lipid vesicle solution: 9 μL of fluorescein loaded GUV solution was put on microscope slide and mixed with 1 μL of appropriate glucose solution (final concentrations of glucose: 0.3, 0.6, 1.2, 2.5, and 5% (w/v)). Samples were incubated at room temperature for up to 10 min and observed with fluorescence microscopy.

e) Addition of ethanol: 9 μL of fluorescein loaded GUV solution was put on microscope slide and mixed with 1 μL ethanol solution (final concentrations of ethanol: 1.2%, 2.5%, 5% and 10%), incubated for up to 10 min and observed with fluorescence microscopy.

f) Changing ionic strength: 9 μL of fluorescein loaded GUV solution was put on microscope slide and mixed with 1 μL of NaCl, $CaCl_2$ or $FeCl_3$ solution (final concentrations of NaCl: 1, 10 and 100 mM; $CaCl_2$: 0.1, 1, 10, and 100 mM; $FeCl_3$: 0.01, 0.1, 1, 10, and 100 mM). Lipid vesicles were incubated for up to 10 min and observed with fluorescence microscopy.

g) Changing pH: 1.2 mL fluorescein loaded GUV solution was put into 15 mL centrifuge tube and pH was adjusted with 0.4 M HCl or NaOH in the range from pH 2 to 12. As the volumes of added HCl or NaOH were small we did not correct for the solution of the lipid vesicles. Lipid vesicles were incubated for up to 10 min and observed with fluorescence microscopy.

h) Fenton reaction: 16 μL of fluorescein loaded GUV solution was put into 1.5 mL microtubes and mixed with 2 μL of H_2O_2 and 2 μL $FeSO_4$ solutions with a molar ratio 1:1, final concentrations of H_2O_2 and $FeSO_4$ were 0.25, 0.5, 1, 2.5, and 5 mM. Samples were incubated in microtubes at room temperature for approximately 10 min. Next, lipid vesicles were observed with fluorescence microscopy.

i) Vortex mixing: 100 μL of fluorescein loaded GUV solution was put into 1.5 mL microtubes and mixed with vortex mixer (IKA MS 3 digital) for 4 min at different rotary speeds: 1000, 2000, and 3000 rpm. Microtube was held in upright position during vortex mixing. Lipid vesicles were immediately observed with fluorescence microscopy. In addition, we have vortex mixed samples with 1.5 mm silica beads. To 100 μL of fluorescein loaded GUV solution in 1.5 mL microtubes 0.1 g of silica beads were added and vortexed at different rotary speeds: 1000, 2000, and 3000 rpm for 4 min.

j) Pipetting: 100 μL of fluorescein loaded GUV suspension was put into 1.5 mL microtubes and 70 μL of sample was repeatedly pipetted with automatic pipette for 100, 500, and 1000 times. Next, lipid vesicles were observed with fluorescence microscopy.

k) Heating: 100 μL of fluorescein loaded GUV suspension was transferred into 1.5 mL microtubes and put into preheated thermoblock heater (Stuart SBH130DC). We incubated samples in a thermoblock for 10 min and cool them down prior to fluorescence microscopy. Lipid vesicle stability was tested at 40, 60, 80, and 100 °C. For long term stability vesicles were stored at room temperature in the dark.

l) Cooling: 100 μL of fluorescein loaded GUV suspension was transferred into 1.5 mL microtubes and put into cold room (4 °C) or frozen at −18 °C and −80 °C. Samples were frozen for approximately 1 h, thawed in hot water (~50 °C), and cooled to room temperature prior to microscopy observation.

m) Electroporation: 100 μL of fluorescein loaded GUV suspension was put into electroporation cuvette with 1 mm gap and transferred into electroporator (Eppendorf 2510). Samples were tested at different electric potential: 800, 1100, 1400, 1700, 2000, 2300, and 2500 V. Discharge time constant was 5 ms with 3.3 kOhm sample impedance. Lipid vesicles were immediately observed with fluorescence microscopy.

n) Microwave: 100 μL of fluorescein loaded GUV suspension was transferred into 1.5 mL microtubes, put into microwave (Daewoo KOR-6185, frequency: 2450 MHz) and heated for 1 min at different output powers (472 W, 623 W and 800 W). After heating, samples were cooled down to room temperature.

o) Shear rate treatment on rheometer: Shear rate experiments were performed on a rotational rheometer Physica MCR 302 (Anton Paar, Graz, Austria) at (25.00 ± 0.01) °C. 70 μL of lipid vesicle suspension was applied to a cone-plate measuring system (CP25) to ensure a constant shear rate within the entire shear gap. The samples were sheared at 2000, 6000, 10000, 14000 and 18500 s^{-1} for 2 min. After shear treatment, lipid vesicles were immediately observed with fluorescence microscopy.

p) Hydrostatic pressure: Specially designed mechanical test rig was made to test static hydrostatic pressure in small liquid volumes. The test chamber was made from stainless-steel rod with hole of 5 mm H5 diameter and 60 mm length. On top of the chamber was piston with diameter of 5 mm H5 which provided displacement to create hydrostatic pressure. Piston had rubber O-ring ϕ5/ϕ1 mm to prevent leakage. Test rig is constructed out of leverage bar and test chamber mounting. Leverage bar was properly weighted to get desired pressure. Drawings of the test rig are presented in Supplementary Fig. S20. We put approximately 900 μL of sample into the testing chamber. Piston was pushed into the chamber to let air and excessive fluid out to obtain same tested volume (working volume was approximately 800 μL). After mounting test chamber into the testing rig, high pressure was applied for 5 min. Applied pressures were: 300, 600, 900, 1200, 1500 and 1800 bar.

q) Ultrasonic cleaning bath: 100 μL of fluorescein loaded GUV suspension was transferred into 1.5 mL microtubes and secured into microcentrifuge floating rack. Ultrasonic cleaning bath (ASonic PRO MED 50, Ultrasonic power: 120 W) was filled with water (water temperature was approx. 21 °C) and samples in floating rack were put into ultrasonic bath. Device has different operating modes – soft and normal modes. Operating frequency was 40 kHz. Samples were sonicated 5 s and 60 s at both operating modes (soft and normal mode). During the sonication, water temperature didn't surpass 25 °C during experiments.

r) Centrifugation: 100 μL of fluorescein loaded GUV suspension was transferred into 1.5 mL microtubes and centrifuged in centrifuge (Eppendorf Centrifuge 5424) for 10 min at different G-forces (10000 × g, 15700 × g, 20000 × g). Before we put sample on microscope slide, we mixed sample with vortex mixer for 10 s at 3000 rpm.

2.3. Stability of fluorescein sodium salt

For all tested conditions, we have checked the stability of fluorescein molecule fluorescence intensity. Fluorescein solution (375 mg/mL) in HEPES buffer was treated the same way as described in section above except that lipids were not added. After treatment, 300 μL of sample was put into 96-wall black microtiter plate with clear bottom. Fluorescence intensity was measured with microplate reader (BioTek Instruments, Inc., Cytation 3, excitation: 500 nm, emission: 530 nm, gain: 50) and compared to the untreated control. Except for the low pH treatment, no decay of fluorescence intensity was observed.

We also tested stability of sodium fluorescein during storage at room temperature in dark. 5 mL of fluorescein solution (375 mg/mL) in HEPES buffer was stored in 15 mL centrifuge tubes. Every 3–4 days, 300 μL of sample was put into 96-wall black microtiter plate with clear bottom and measured fluorescence. Fluorescence intensity was measured with microplate reader (BioTek Instruments, Inc., Cytation 3, excitation: 500 nm, emission: 530 nm, gain: 50).

2.4. Fluorescence microscopy

The samples with fluorescein loaded giant unilamellar vesicles were visualized on fluorescence microscope Zeiss Axio Observer Z1 equipped with confocal unit LSM 800. Samples were prepared for microscopy with the following procedure: all samples were first vortex mixed for 5 s (at 3000 rpm), then 10 μL of untreated or treated sample was put on microscope slides, covered with 20 × 20 mm cover glass and sealed with VALAP vax (vaseline, lanolin, paraffin). Microscopic images were taken on 20x/0.4NA objective with 488 nm laser at 0.48% laser intensity. Pinhole was set to 100 μm (1.9 Airy Units ~11.3 μm thick section). Emission range was set 400–647 nm. Image acquisition mode was tiles imaging (2 × 2 tiles) on 5 random places on microscopic glass (on each corner of cover glass and one in the centre of sample). Single (2 × 2 tiled) image covered 1213.9 × 1213.9 μm of sample area. Acquired image frame size was 1024 × 1024 pixel. Pixel dwell time was 0.76 μsec, scan time 1.86 sec (scan speed was 8, averaging was set on number 2, digital magnification 0,5×).

2.5. Analysis of microscopic images

Microscopic images were analysed with ImageJ 1.52i software. We set threshold to discriminate lipid vesicles from the background of the images and analysed with Particle analyser (set parameters: size = 4–100, circularity = 0.50–1.00). We obtained vesicle area and mean vesicle fluorescence intensity.

2.6. Calculation of lipid vesicle parameters

To obtain fluorescence intensity of the individual vesicle the following corrections were performed: (i) fluorescence intensity of HEPES buffer was subtracted from mean fluorescence intensity of each vesicle, (ii) the background was further reduced by subtracting the image background value as obtained by “subtract background” function of ImageJ. As this value represents the background of the whole optical section void of vesicles, we have weighted its contribution relative to the thickness of space in z-direction not occupied by the vesicle. For example, the obtained fluorescence intensity of vesicle with 6 μm diameter in an image of 10 μm optical thickness has two contributions: fluorescence from background that originates from 4 μm thick void space and fluorescence from 6 μm thick vesicle, therefore 40% of background fluorescence value obtained from the background void of vesicles was included in vesicle fluorescence intensity correction. The vesicle diameter was calculated from vesicle area, by assuming the spherical shape of the vesicle. To obtain fluorescence intensity per unit volume, the fluorescence intensity of the vesicle was normalized by vesicle diameter. In the results the diameter normalized fluorescence intensity was calculated as an average over all vesicles and is presented as an average vesicle fluorescence. To calculate fluorescein amount per vesicle the diameter normalized fluorescence intensity was multiplied by vesicle volume. The total fluorescence for vesicles, as shown in the results, was obtained by summing fluorescence intensity of the individual vesicles.

The acquired confocal microscopic images had an optical slice thickness of 11.3 μm, thus only vesicles with diameters 11.3 μm or less (~98% of all vesicles) were included in the analysis. The vesicles with diameters < 2.4 μm were indistinguishable from the noise and were thus not included in the analysis. All results are represented relative to the untreated samples (controls).

2.7. Data fitting

Results for long-term stability of fluorescein loaded GUV at room temperature in the dark over time were statistically analysed with Origin software. Each independent sample fluorescence intensity was first normalized to the initial state (day 0), next we fitted the normalized results with the exponential decay function (ExpDec1 function).

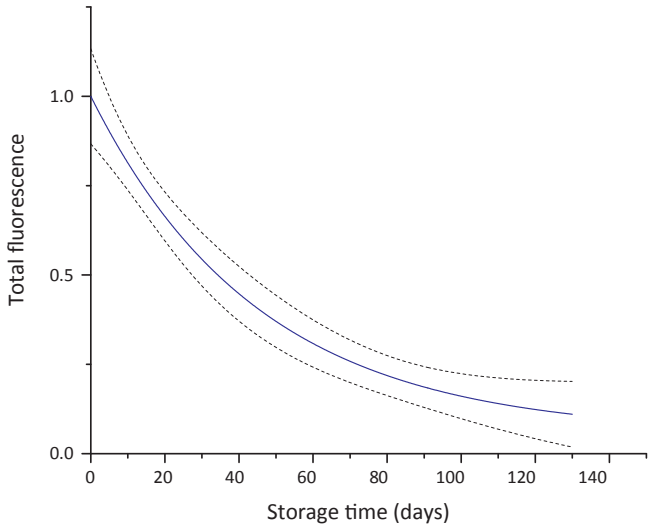

Fig. 1. GUV stability of DOPC at room temperature, stored in dark. Blue line represents an exponential decay function fitted to the normalized total fluorescence of fluorescein loaded vesicles during storage. Grey dashed lines represent 95% confidential interval (n = 3). (For interpretation of the references to colour in this figure legend, the reader is referred to the web version of this article.)

3. Results

The long-term stability of DOPC giant unilamellar vesicles (GUV) loaded with fluorescein stored in the dark at room temperature is given in Fig. 1. The total fluorescence decreased exponentially. The average decay time, the time when the initial fluorescence decreased to 1/e was (31.5 ± 8.5) days. Fluorescence intensity of the control fluorescein solution after 110 days of storage did not decrease significantly suggesting that the decrease of fluorescence intensity in GUV was not due to fluorescein decay. All the experiments on lipid vesicle stability were done on freshly prepared GUV and the duration of experiment with various physico-chemical stressors did not exceed 60 min. We therefore assumed that leakage and decay of fluorescein from untreated GUV was negligible. To compare the effect of different physico-chemical stressors on lipid vesicle stability all the results were normalized to the fluorescence intensity of the non-treated control GUV samples.

Hydrodynamic cavitation (HC) was recently introduced as method of choice to destroy bacteria [33–36]. Here we have tested for the first time the effect of HC on giant lipid vesicles as a model system for bacterial lipid bilayers. We have designed a new small volume hydrodynamic device (Supplementary Fig. S21) with Venturi restriction. The stability of GUV lipid vesicles treated with HC is shown in Fig. 2. A polydisperse distribution of vesicle size was observed before HC treatment. After 100 passes through Venturi restriction, only few small sized GUVs remained. The increase of background fluorescence, due to the leakage of fluorescein to the surrounding, was not measurable on fluorescent micrographs as it was below the detection limit of the microscope.

To further characterize the effect of HC on lipid vesicles, we analysed the individual lipid vesicles on microscopic images. The total fluorescence intensity, vesicle number, vesicle volume and vesicle fluorescence intensity of GUV relative to the untreated control sample are given in Fig. 3A. The results show that after 100 passes, the average lipid vesicles number, volume and total fluorescence intensity significantly decreased. Reduction in vesicle diameter is presented in Fig. 3B, where can be seen shift of vesicle size distribution toward

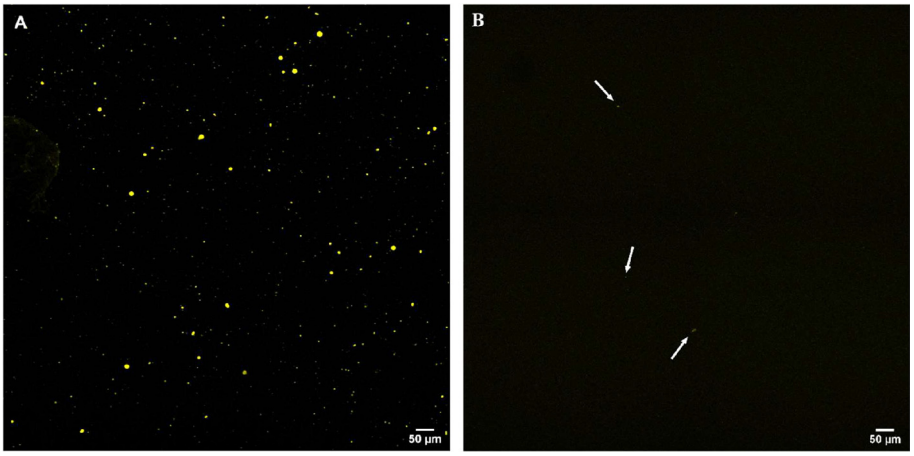

Fig. 2. Fluorescence microscopic images of DOPC vesicles labelled with fluorescein before (A) and after hydrodynamic cavitation treatment – 100 passes (B). Yellow objects represent fluorescein labelled vesicles of different sizes. Arrows in panel B indicate few small sized lipid vesicles that remained after hydrodynamic cavitation treatment. (For interpretation of the references to colour in this figure legend, the reader is referred to the web version of this article.)

smaller vesicles size. There was small, but significant fraction of lipid vesicles that resist the hydrodynamic treatment. The average vesicle fluorescence intensity of the remaining vesicles did not change significantly relative to the untreated vesicles.

Cavitation bubbles can also be generated with propagation of acoustic waves through the liquid medium [59]. Application of low amplitude (3 µm) ultrasound did not cause a major leak of fluorescein from the GUV (Fig. 4). With increasing amplitude, however, the total fluorescence decreases exponentially. At 12 µm amplitude the majority of GUV were empty of fluorescein or destroyed. As given in Fig. 4 the number of GUV, the average volume of the remaining fluorescein labelled GUV, as well as the average liposome fluorescence decreased with increasing ultrasound amplitude. This indicates a disruption of the giant lipid vesicles at high amplitude treatments. The size distribution analysis of lipid vesicles (Fig. 4E) suggests that with increasing ultrasound amplitude the size distribution of GUV moved towards smaller sized vesicles. Consistently, the number of GUV independently determined by DIC microscopy also decreased. The decrease of the number of vesicles determined with DIC correlated with the number of lipid vesicles determined by fluorescence. This implies that the decrease of the total fluorescence intensity in GUV was mainly due to vesicle disintegration. Compared to ultrasound applied by sonotrode, lipid vesicles treated with ultrasonic bath showed less effect on vesicles integrity (Supplementary Fig. S1). Increasing power output of the ultrasonic bath had similar effect to increasing amplitude of sonotrode.

The effects of different chemistry on GUV stability are given in Fig. 5. Only the highest concentrations used are shown in Fig. 5. The effect of other concentrations are given in Supplementary material (Fig. S2 – S6). Lipid vesicles were not resistant to osmolarity change. Compared to the untreated control ~40% of fluorescein leaked out of lipid vesicles treated with 5% (w/v) glucose. Vesicles treated with 10% ethanol or 100 mM NaCl and $CaCl_2$ leaked even more fluorescein. Most of the GUV were disrupted upon addition of 100 mM $FeCl_3$. When we induced free radical formation with Fenton reaction by mixing 2.5 mM $FeSO_4$ with 2.5 mM H_2O_2 lipid vesicles disintegrated instantly. The addition of either 2.5 mM $FeSO_4$ or 2.5 mM H_2O_2 to the GUV did not cause lipid vesicle disintegration (Supplementary Fig. S6).

It is surprising that the addition of 100 mM Fe^{3+} ions had such a dramatic effect on GUV stability, in particular when compared to the addition of monovalent and divalent cations. It is known that the addition of ferric iron induces water hydrolysis and may significantly decrease pH [60]. The pH of 100 mM $FeCl_3$ solution was 1.9. This is very low and may have an effect on zwitterionic DOPC vesicles and fluorescence intensity of fluorescein marker [61,62]. To check this, we have measured fluorescein stability at different pH values. In Supplementary Fig. S7 we show that fluorescein is stable above pH 7.4, however at low pH fluorescein molecule decays. We have also changed the pH of lipid vesicle suspension. The results for total fluorescence are given only for pH 7.4 or higher (Supplementary Fig. S8). DOPC vesicles were most stable at pH 7.4. Increasing pH decreased the amount of total fluorescence in the vesicles as well as the number of fluorescein vesicles. The effect of low pH has been tested with DIC microscopy. We have observed a significant decrease of the number of lipid vesicles which suggest that also low pH has a significant effect on DOPC lipid GUV stability.

Solubilization of GUV with Triton X-100 is given in Supplementary Fig. S9. At low concentrations of Triton X-100, below the critical micellar concentration, the addition of detergent did not significantly

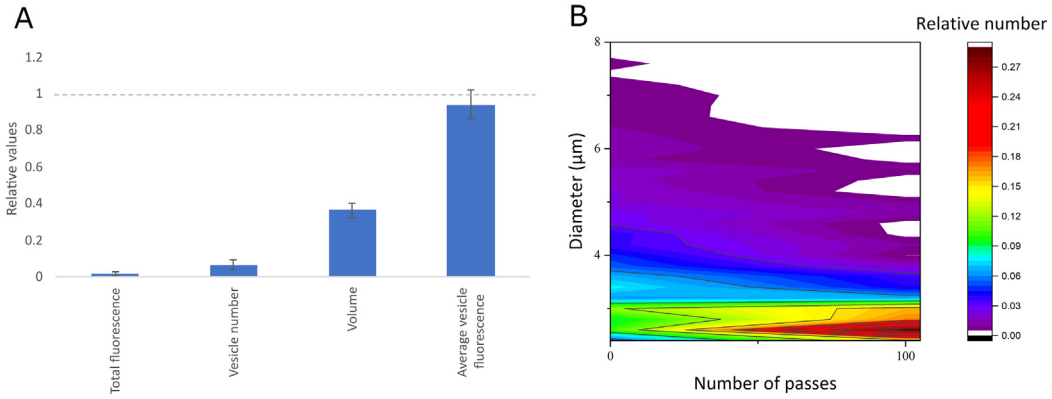

Fig. 3. Treatment of DOPC GUV with hydrodynamic cavitation. Panel A shows relative values of total fluorescence, the average vesicle number, vesicle volume and vesicle fluorescence relative to the untreated control, which is represented by dashed line (—). Panel B shows size distribution of individual fluorescein loaded vesicles during the hydrodynamic cavitation treatment. Average values and standard error are given in panel A (n = 5).

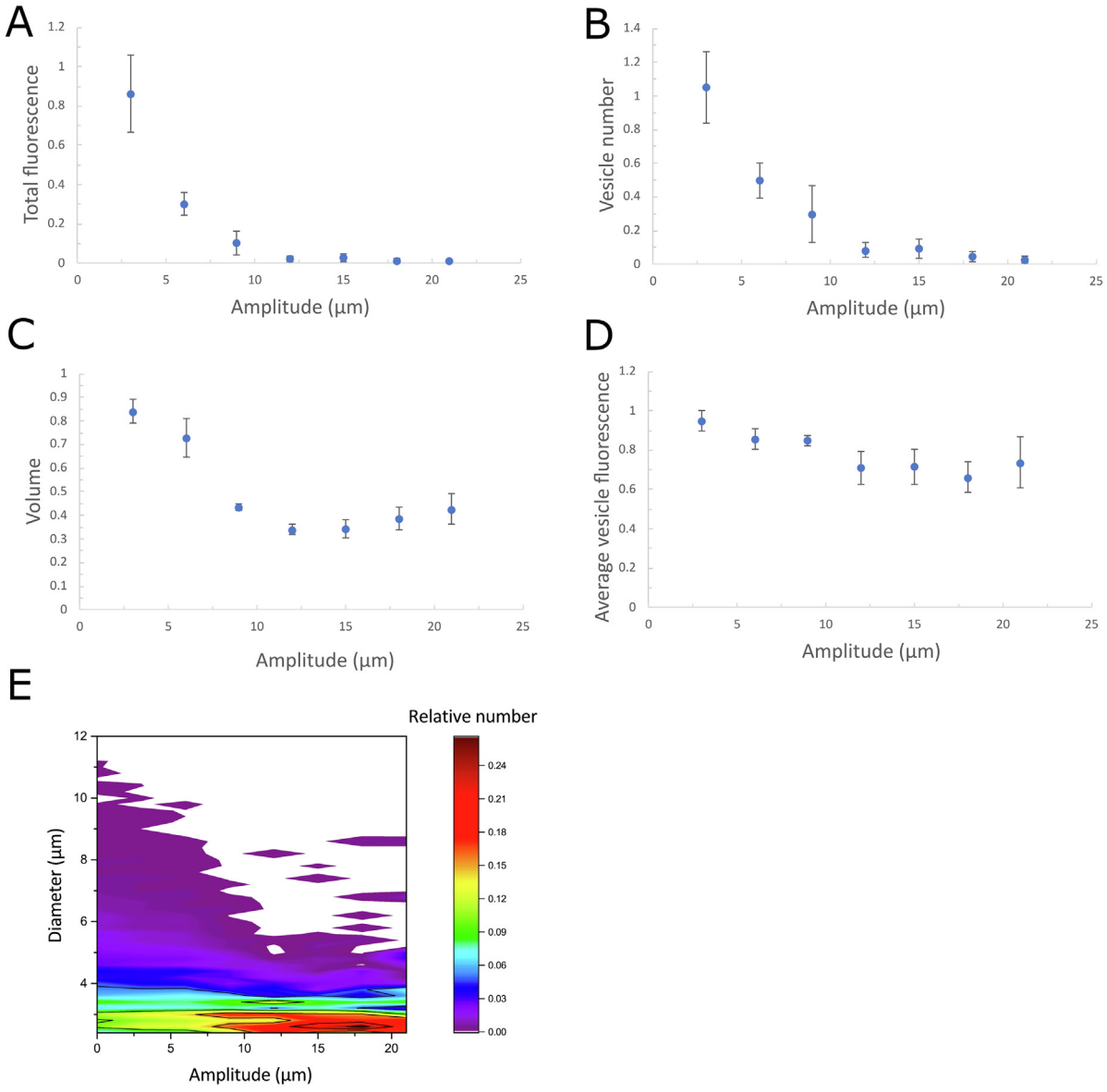

Fig. 4. The effect of different ultrasound amplitude on the total fluorescence of vesicles (A), relative number of fluorescein loaded vesicles (B), the average volume of the remaining vesicles (C), the average vesicle fluorescence of the remaining vesicles (D), and the vesicle size distribution at different amplitudes of ultrasound (E). The results in A–D represent the total fluorescence of vesicles, average number, volume and vesicle fluorescence relative to the untreated control, represented by value of 1. The average values and standard errors (n = 4) are given for A-D.

compromised lipid vesicle stability. However, with increasing detergent concentration vesicles were progressively disrupted. At first the volume of lipid vesicles increased compared to untreated vesicles, most notably at 0.85 mM Triton X-100. The number of remaining lipid vesicles above the critical micellar concentration decreased drastically. We have observed that Triton X-100 first solubilized small sized GUV followed by disruption of larger vesicles at higher detergent concentrations (Supplementary Fig. S9E).

In addition to chemical stressors the GUV were exposed to different mechanical treatments as well (Fig. 6). Only the effect of the largest magnitude for a given stressor is given in Fig. 6. The effects for lower magnitudes are given in the Supplementary information. Pipetting lipid vesicle suspension several times had little effect on lipid integrity. If the number of pipetting was increased to unrealistically high number, i.e. 500 times or higher (Supplementary Fig. S10), small effect on lipid stability was observed. On the other hand, when shear stress was increased by vortexing, surprisingly, the total fluorescence increased relative to the untreated control. Since the relative average vesicle volume and average vesicle fluorescence did not change, but the number of vesicles increased (Supplementary Fig. S11), it is likely that during vortexing more lipid vesicles were resuspended compared to the untreated control lipid vesicle suspension. If shear stress during vortexing was further increased by adding glass beads, vesicles were destroyed (Supplementary Fig. S12). We also applied rotational shear stress on lipid vesicle solution with rotational rheometer up to shear rate of 18500 s^{-1}. Although this is considered to be a high shear rate, no significant effect on vesicle integrity was observed (Supplementary Fig. S13).

The electroporation had a strong effect on vesicle integrity and significantly decreased the total fluorescence and the number of vesicles. As given in Supplementary Fig. S14 the effect on vesicle volume, and average vesicle fluorescence was less pronounced. Increased temperature decreased lipid vesicle integrity only at temperatures above 80 °C. Similarly freeze-thawing decreased the total fluorescence and volume but has less effect on the number and average vesicle fluorescence (Supplementary Fig. S15). The effect of static pressure on lipid

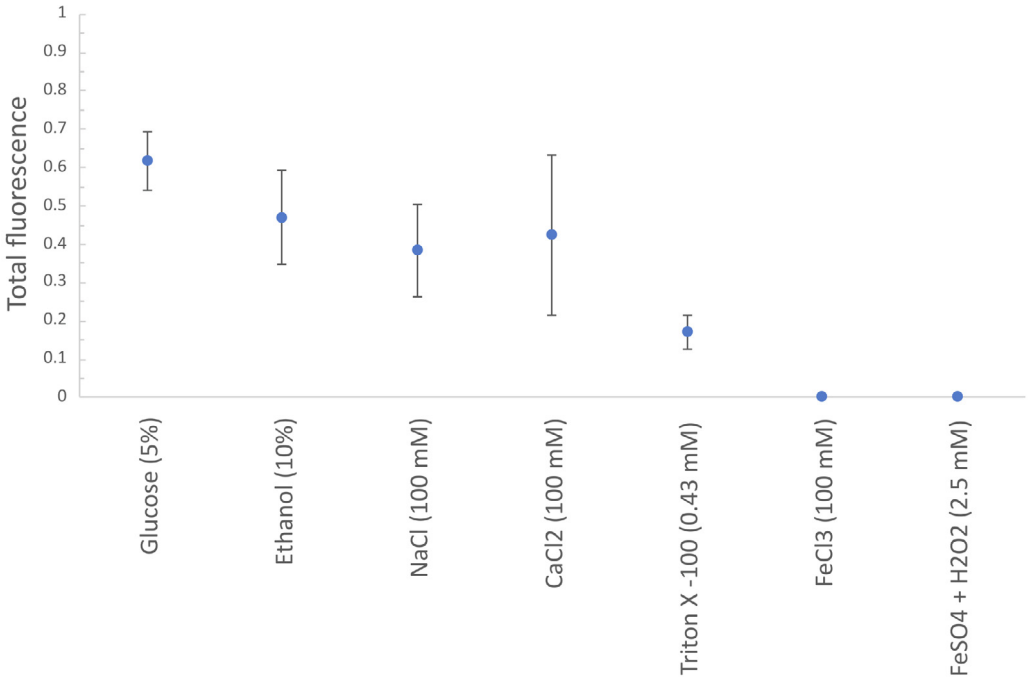

Fig. 5. The effect of different chemical treatments on DOPC integrity. The relative total fluorescence intensity is normalized relative to control untreated samples. Average values and standard errors are given (n = 4 or 5).

stability is given in Supplementary Fig. S16, where it can be seen that vesicles are fairly stable to high pressures. Vesicle destruction can only be seen at pressures higher than 1200 bar. The effect of microwave treatment is given in Supplementary Fig. S17. The results suggest that microwaves induce leakage of fluorescein from the vesicles. The effect was dependent on the microwave output power. Microwaves did not have an effect on the number and volume of vesicles, but significantly decreased average vesicle fluorescence. One of the most frequently used technique in the laboratory is centrifugation. The results of centrifugation on vesicle stability are given in Supplementary Fig. S18. With increasing g force lipid vesicles progressively leaked more. However, the effect of centrifugation was moderate.

The 3D comparison of lipid vesicle stability to different physicochemical and mechanical forces relative to the untreated lipid vesicles

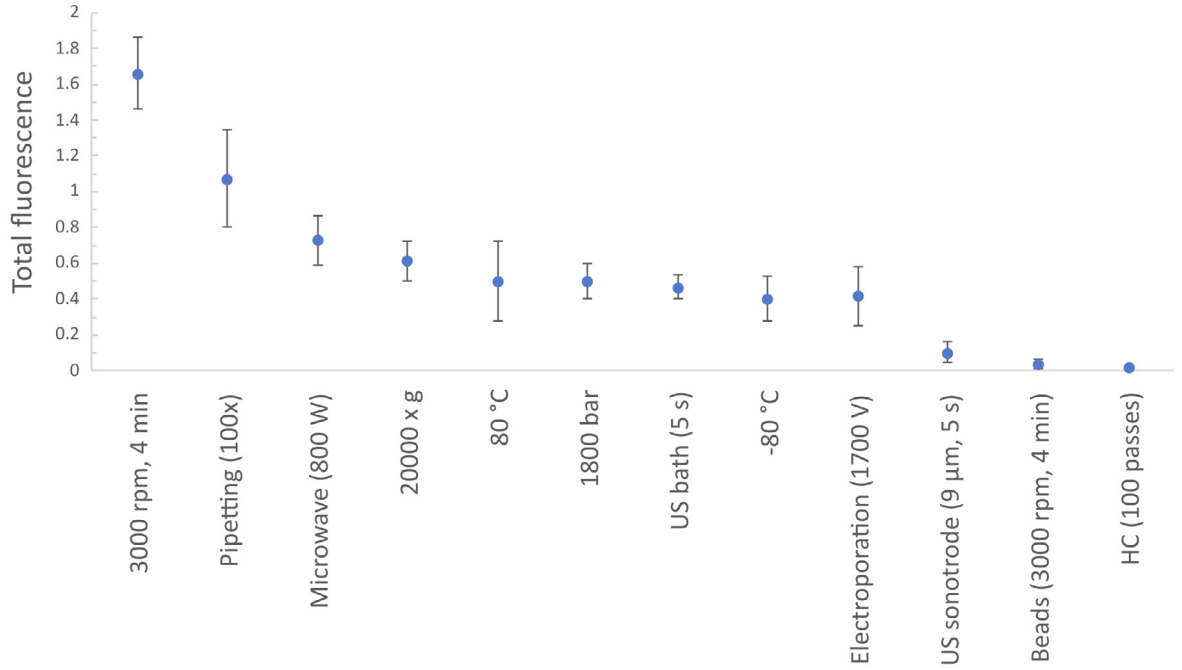

Fig. 6. DOPC vesicle integrity upon different mechanical and physical treatments of vesicles. The relative total fluorescence intensity after treatment compared to fluorescence intensity before treatment. Standard errors are given (n = 4). Shown parameters from left to right: vortex mixing (3000 rpm, 4 min), pipetting (100x), microwave irradiation (output power 800 W), centrifugation (20000 × *g*, 10 min), heating (80 °C), high pressure (1800 bar), ultrasonic bath (40 kHz, 5 s) freezing-thawing (−80 °C), electroporation (1700 V), ultrasonication with sonotrode (9 µm amplitude, 5 s), vortex mixing with beads (3000 rpm, 4 min), hydrodynamic cavitation (100 passes).

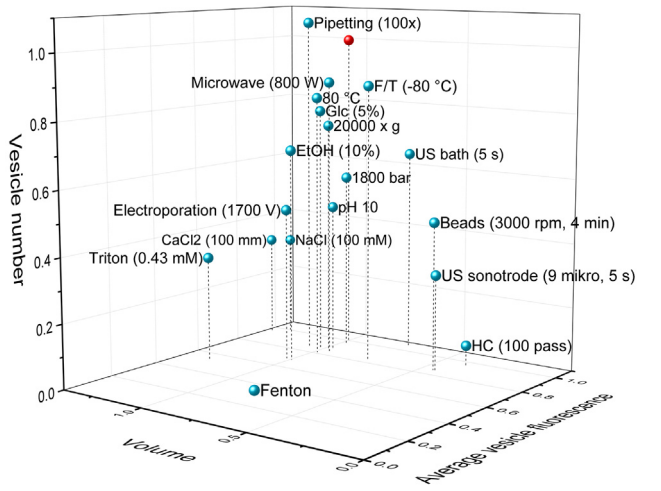

Fig. 7. Summary of relative importance of different environmental stressors on lipid vesicle stability. The data represent values of average vesicle volume, average vesicle fluorescence and number of vesicles relative to the untreated control. Red dot on graph represents the untreated control (all values are equal to 1.0). Abbreviations: F/T (−80 °C) – freezing-thawing at −80 °C; 80 °C – heating on 80 °C; glc (5%) – glucose (5%); 20000 × *g* – centrifugation at 20000 × *g*; EtOH (10%) – ethanol (10%); 1800 bar – high pressure (1800 bar); beads (3000 rpm, 4 min) – vortex mixing with beads at 3000 rpm for 4 min; HC (100 passes) – hydrodynamic cavitation (100 passes); Fenton – $FeSO_4$ + H_2O_2 (2.5 mM). (For interpretation of the references to colour in this figure legend, the reader is referred to the web version of this article.)

for the worst-case scenario (i.e. the highest magnitude of the parameter used in this study) is given in Fig. 7. Several 2D slices such as vesicle volume : fluorescence, volume : number, and vesicle fluorescence : number are given in Supplementary Fig. S19. Vesicles responded to different environmental stressors either by changing volume, intravesicular fluorescein concentration, the number of vesicles, or a combination of this parameters.

This suggests that there are several mechanisms at work in decreasing lipid vesicle stability. Compared to other stressors, HC is a very effective method for lipid vesicle disintegration. It effectively decreases the number and size of lipid vesicles. The effect of hydrodynamic treatment on lipid vesicles is comparable to the effect of ultrasound with more pronounced decrease of vesicle number and higher fluorescence intensity of the remaining vesicles. HC reduces the number of lipid vesicles as effectively as free radicals; however, the volume of the remaining vesicles is smaller with higher fluorescence intensity.

4. Discussion

The field of liposome research is immense. Due to their biological significance (i.e. bacterial membrane model system) and applications in different industries and medicine lipid vesicles and their stability remain an active area of research. In this study we have used hydrodynamic cavitation to destroy lipid vesicles and compared its effect to other chemical, physical and mechanical treatments. By normalizing different treatments to untreated control, we were able to compare the effect of different physico-chemical treatments on vesicle stability. The results clearly demonstrate that hydrodynamic cavitation is a very effective treatment method to destroy lipid vesicles. In the following we discuss different mechanisms of liposome destruction in order to infer possible mechanisms of lipid vesicle destruction by hydrodynamic cavitation.

One can imagine several mechanisms of lipid vesicle disruption that induce leakage of fluorescein from vesicles. Vesicles can become transiently porous and leak fluorescein with no substantial volume change during the process (e.g. electroporation). Lipid pores may form on a longer timescale and grow to a critical size that leads to disintegration of lipid vesicle into several fragments that reassemble into smaller vesicles (e.g. shear stress). Lipid vesicle may buckle by shear stress and fragment to smaller vesicles. The ultimate disruption of lipid vesicles is solubilisation with surface active molecules (e.g. Triton X-100). Depending on the physico-chemical treatment, different combinations of the above-mentioned processes may occur in lipid vesicles disruption.

The results of this study indicate that all treatments tested had an effect on lipid stability either by decreasing lipid vesicle number, volume, fluorescence intensity or a combination of these parameters. The effect of salts, solvents, surface active agents, free radicals, temperature, and pressure on lipid vesicle stability have been well documented in the literature. Because our results do not deviate strongly from the published data they will not be further discussed. Much less, however, is known about the effect of high shear stress, centrifugation, vortex mixing, microwaves or hydrodynamic cavitation. The effect of shear stress was strongly dependent on the treatment applied. For example, pipetting had a negligible effect on lipid vesicle stability unless repeated at unrealistically high numbers. Lipid vesicles were stable in the shear rate range from 0 to 18500 s^{-1} on rotational rheometer. It has been demonstrated for the dilute and semi dilute regime that the rheological behaviour of small unilamellar DMPC bilayer vesicles is similar to that of a hard-sphere dispersion [63]. Although the tested shear rate range was rather large the results suggest that lipid vesicles do not deform sufficiently to allow for fluorescein leakage. Pal and Khakhar [64] showed size reduction of liposomes during constant shear stress (4000 s^{-1}) only after 6 h of applied shear stress. The proposed mechanism behind vesicle size reduction was deformation and rupture of vesicles above the critical diameter into smaller sized vesicles. They suggested that the breakage process was stochastic, since not all vesicles larger than critical diameter did not rupture.

The effect of microwave irradiation on lipid vesicle stability was significant. Already after one minute of treatment we have observed fluorescein leakage from lipid vesicles. The effect increased with increasing microwave power output. Saalman et al. [65] have showed that 2.45 GHz microwave irradiation significantly increased membrane permeability. Also, Orlando et al. [66] reported similar observations. In these experiments, however, lipid vesicles were subjected to long exposure times (several hours), whereas we exposed treated samples to microwave irradiation only for a short time.

The most detrimental mechanical treatments for lipid vesicles were vortex mixing with glass beads, ultrasound and hydrodynamic cavitation. The effect of vortex mixing was strongly increased when glass beads were added to the lipid solution. The number of vesicles and the volume of vesicles decreased significantly already after 4 min of vortex mixing with beads. Interestingly the fluorescence intensity of the remaining lipid vesicles decreased only slightly. This indicates that upon vigorous vortex mixing with glass beads lipid vesicles disintegrate and reseal to smaller vesicles almost instantaneously with no significant loss of fluorescein in the remaining vesicles.

Both, ultrasound and hydrodynamic treatment produced bubbles. During cavitation, when the bubble violently collapses extreme environmental conditions may be present. In collapsing bubble so called “hot spots” (~4500 K [39]) are created, it is expected that high shear stress exist during microjet bursts (shear rate in excess of 100000 s^{-1} [67], high fluid velocities ~100 m/s [40]), with resultant pressure waves and formation of free radicals. The collapse of bubbles during sonication is frequently correlated with the formation of free radicals [42]. Formation of highly reactive free radicals is very effective for vesicle disintegration as free radicals oxidize phospholipids. Our results for free radicals are consistent with the notion that oxidation of lipid bilayers leads to pore formation, destabilization and disintegration of bilayers [68]. Nevertheless, the exact mechanism of lipid vesicle disruption by ultrasound is still unknown. It is expected that low frequency ultrasound induces vesicle leakage by sonoporation due to pressure

oscillations and cavitation effects [69–71]. Ultrasound induced pores reseal as soon as the ultrasound is ceased and leakage from the vesicles stops [31,70,72,73]. Whereas most pores would be transient, allowing molecular transport before healing, some pores may grow to a critical size and cause liposome destruction [31,74]. In general terms our results are consistent with pore formation and fragmentation to smaller size vesicles upon ultrasound treatment. It has been reported that higher sonication frequencies cause vesicle reduction to smaller diameters [75]. Size distribution of vesicles in our experiments shifted towards smaller size with increasing amplitude of ultrasound. This is in agreement with the fact that ultrasound is used to prepare small unilamellar vesicles from large multilamellar vesicles [69,76]. Although our results agree with this findings there were some inconsistencies. Most notably a subpopulation of vesicles was resistant to sonication and even at increased ultrasound amplitude there was only a limited change of volume or leakage from the resistant vesicles. The volume of resistant vesicles unexpectedly slightly increased at higher amplitudes.

Similar cavitation phenomena may be induced by hydrodynamic cavitation. In this case, it is the acceleration of the fluid flow which causes local pressure to drop and induces bubble formation [38]. Although in principle both sono and hydrodynamic cavitation induce bubble formation the effects may differ (i.e. number of pressure pulses and cavitation intensity) [77,78]. We have induced cavitation bubble formation in a hydrodynamic flow with Venturi restriction. Results imply that hydrodynamic cavitation has a dramatic effect on vesicle stability comparable in magnitude to the effect of sonication, vortex mixing with glass beads, and free radicals. It proceeds from large vesicles to progressively smaller vesicles. The transformation from large to small vesicles must be fast as the remaining vesicles have approximately the same amount of fluorescein as untreated vesicles, which suggest a quick resealing of disrupted vesicles.

Application of sonication is widely used as cleaning or dispersing mechanism [79–81], on the other hand hydrodynamic cavitation is less commonly applied but much easier to induce. However, this is changing rapidly as many different applications of hydrodynamic cavitation are emerging nowadays [82–84]. Here, we showed for the first time that hydrodynamic cavitation is a powerful new tool to destroy lipid bilayers. Because lipid bilayer integrity is crucial for cell viability it is possible that reported bacterial inactivation by hydrodynamic cavitation is at least in part due to membrane disruption [48]. It remains to be seen if the disruption of membrane in more complex systems (i.e. bacterial spheroplast which lack bacterial cell wall or bacterial cells) by hydrodynamic cavitation is also very effective.

5. Conclusions

The experimental survey of a large collection of environmental stressors, among them many that have not been described yet in the literature demonstrate both extraordinary robustness of lipid vesicles to environmental challenges (i.e. high resistance to static pressure) as well as extreme fragility to hydrodynamic cavitation, ultrasound, free radicals or vortex mixing with glass beads. The results also demonstrate that fluorescence approach, based on individual lipid vesicle fluorescence intensity, can successfully describe lipid vesicle stability. By focusing our research to a single lipid vesicle composition, to giant unilamellar lipid vesicles size class, to a single method of preparation and detection we have obtained a consistent set of data that allowed us to compare the relative magnitude of different stressors on lipid vesicle stability. Based on the results we conclude that hydrodynamic cavitation is a highly effective method to destroy liposomes.

Acknowledgments

The authors acknowledge the financial support from the European Research Council (ERC) under *the European Union's* Framework Program for research and innovation, Horizon 2020 (grant agreement n° *771567 — CA*BUM) and the Slovenian Research Agency (research core funding No. P2-0401 and P4-0116). We would like to thank Mr. Tone Godeša for producing hydrostatic pressure test rig.

Appendix A. Supplementary data

Supplementary data to this article can be found online at https://doi.org/10.1016/j.ultsonch.2019.104826.

References

[1] L.E. Locascio, W.N. Vreeland, A. Jahn, M. Gaitan, Liposomes as model cellular systems: liposome formation and applications in microfluidics, Lab-on-Chips for Cellomics (2007) 59–81, https://doi.org/10.1007/978-1-4020-2975-2_3.
[2] S. Talegaonkar, P. Mishra, R. Khar, S. Biju, Vesicular systems: an overview, Indian J. Pharm. Sci. 68 (2006) 141, https://doi.org/10.4103/0250-474X.25707.
[3] Y.-H.M. Chan, S.G. Boxer, Model Membrane Systems and Their Applications State of the field, Curr. Opin. Chem. Biol. 11 (2007) 581–587 https://www.ncbi.nlm.nih.gov/pmc/articles/PMC2196400/pdf/nihms35927.pdf.
[4] B.N. Rao, K.R. Reddy, B. Mounika, S.R. Fathima, A. Tejaswini, Vesicular Drug Delivery System : A Review 12 (2019) 39–53.
[5] C.G. Siontorou, G.P. Nikoleli, D.P. Nikolelis, S.K. Karapetis, Artificial lipid membranes: past, present, and future, Membranes (Basel) 7 (2017) 1–24, https://doi.org/10.3390/membranes7030038.
[6] G. Gregori, S. Citterio, A. Ghiani, M. Labra, S. Sgorbati, S. Brown, M. Denis, Resolution of Viable and Membrane-Compromised Bacteria in Freshwater and Marine Waters Based on Analytical Flow Cytometry and Nucleic Acid Double Staining, Appl. Environ. Microbiol. 67 (2001) 4662–4670, https://doi.org/10.1128/AEM.67.10.4662-4670.2001.
[7] F. Ou, C. McGoverin, S. Swift, F. Vanholsbeeck, Rapid and cost-effective evaluation of bacterial viability using fluorescence spectroscopy, Anal. Bioanal. Chem. (2019), https://doi.org/10.1007/s00216-019-01848-5.
[8] M. Berney, F. Hammes, F. Bosshard, H.-U. Weilenmann, T. Egli, Assessment and interpretation of bacterial viability by using the LIVE/DEAD BacLight Kit in combination with flow cytometry, Appl. Environ. Microbiol. 73 (2007) 3283–3290, https://doi.org/10.1128/AEM.02750-06.
[9] L. Boulos, M. Prévost, B. Barbeau, J. Coallier, R. Desjardins, LIVE/DEAD(®) BacLight(TM): Application of a new rapid staining method for direct enumeration of viable and total bacteria in drinking water, J. Microbiol. Methods. 37 (1999) 77–86, https://doi.org/10.1016/S0167-7012(99)00048-2.
[10] S.M. Stocks, Mechanism and use of the commercially available viability stain, BacLight, Cytom. Part A 61 (2004) 189–195, https://doi.org/10.1002/cyto.a.20069.
[11] A. Laouini, C. Jaafar-Maalej, I. Limayem-Blouza, S. Sfar, C. Charcosset, H. Fessi, Preparation, Characterization and Applications of Liposomes: State of the Art, J. Colloid Sci. Biotechnol. 1 (2012) 147–168, https://doi.org/10.1166/jcsb.2012.1020.
[12] K. Shashi, K. Satinder, P. Bharat, A complete review on: liposomes, Int. Res. J. Pharm. 3 (2012).
[13] N. Bavi, Y. Nakayama, O. Bavi, C.D. Cox, Q.-H. Qin, B. Martinac, Biophysical implications of lipid bilayer rheometry for mechanosensitive channels, Proc. Natl. Acad. Sci. 111 (2014) 13864–13869, https://doi.org/10.1073/pnas.1409011111.
[14] H. Wang, J. de Joannis, Y. Jiang, J.C. Gaulding, B. Albrecht, F. Yin, K. Khanna, J.T. Kindt, Bilayer Edge and Curvature Effects on Partitioning of Lipids by Tail Length: Atomistic Simulations, Biophys. J. 95 (2008) 2647–2657, https://doi.org/10.1529/biophysj.108.131409.
[15] T. Shigematsu, K. Koshiyama, S. Wada, Line tension of the pore edge in phospholipid / cholesterol bilayer from stretch molecular dynamics simulation 11 (2016) 1–10, https://doi.org/10.1299/jbse.15-00422.
[16] L. Tayebi, D. Vashaee, A.N. Parikh, Stability of Uni- and Multillamellar Spherical Vesicles, ChemPhysChem. 13 (2012) 314–322, https://doi.org/10.1002/cphc.201100573.
[17] T.J. Pucadyil, S. Mukherjee, A. Chattopadhyay, Organization and dynamics of NBD-labeled lipids in membranes analyzed by fluorescence recovery after photobleaching, J. Phys. Chem. B. 111 (2007) 1975–1983, https://doi.org/10.1021/jp066092h.
[18] Science 175 (4023) (1972) 720–731, https://doi.org/10.1126/science:175.4023.720.
[19] J.D. Nickels, J.C. Smith, X. Cheng, Lateral organization, bilayer asymmetry, and inter-lea fl et coupling of biological, membranes 192 (2015) 87–99.
[20] M. Repetto, J. Semprine, A. Boveris, Lipid Peroxidation: Chemical Mechanism, Biological Implications and Analytical Determination, Lipid Peroxidation (2012) 3–30, https://doi.org/10.5772/45943.
[21] M.P. Goertz, N. Goyal, G.A. Montano, B.C. Bunker, Lipid Bilayer Reorganization under Extreme pH Conditions (2011) 5481–5491, https://doi.org/10.1021/la2001305.
[22] W.W. Sułkowski, D. Pentak, K. Nowak, A. Sułkowska, The influence of temperature, cholesterol content and pH on liposome stability, J. Mol. Struct. 744–747 (2005) 737–747, https://doi.org/10.1016/j.molstruc.2004.11.075.
[23] M.M. Koerner, L.A. Palacio, J.W. Wright, K.S. Schweitzer, B.D. Ray, H.I. Petrache, Electrodynamics of lipid membrane interactions in the presence of zwitterionic buffers, Biophys. J. 101 (2011) 362–369, https://doi.org/10.1016/j.bpj.2011.05.

062.
[24] N. Kato, A. Ishijima, T. Inaba, F. Nomura, S. Takeda, K. Takiguchi, Effects of Lipid Composition and Solution Conditions on the Mechanical Properties of Membrane Vesicles (2015) 22–47, https://doi.org/10.3390/membranes5010022.
[25] M.M.A.E. Claessens, B.F. Van Oort, F.A.M. Leermakers, F.A. Hoekstra, M.A.C. Stuart, Charged lipid vesicles: Effects of salts on bending rigidity, stability, and size, Biophys. J. 87 (2004) 3882–3893, https://doi.org/10.1529/biophysj.103.036772.
[26] A. Kodama, M. Morandi, R. Ebihara, T. Jimbo, M. Toyoda, Y. Sakuma, M. Imai, N. Pu, M.I. Angelova, Migration of Deformable Vesicles Induced by Ionic Stimuli (2018), https://doi.org/10.1021/acs.langmuir.8b02105.
[27] J. De Gier, J.G. Mandersloot, L.L.M. Van Deenen, Lipid composition and permeability of liposomes, Biochim. Biophys. Acta - Biomembr. 150 (1968) 666–675, https://doi.org/10.1016/0005-2736(68)90056-4.
[28] H. Sakai, T. Gotoh, T. Imura, K. Sakai, K. Otake, M. Abe, Preparation and Properties of Liposomes Composed of Various Phospholipids with Different Hydrophobic Chains Using a Supercritical Reverse Phase Evaporation Method 621 (2008) 613–621, https://doi.org/10.5650/jos.57.613.
[29] C.R. Kensil, E.A. Dennis, Alkaline hydrolysis of phospholipids in model membranes and the dependence on their state of aggregation, Biochemistry 20 (1981) 6079–6085, https://doi.org/10.1021/bi00524a025.
[30] M. Grit, D.J.A. Crommelin, Chemical stability of liposomes: implications for their physical stability, Chem. Phys. Lipids. 64 (1993) 3–18, https://doi.org/10.1016/0009-3084(93)90053-6.
[31] P. Marmottant, T. Biben, S. Hilgenfeldt, Deformation and rupture of lipid vesicles in the strong shear flow generated by ultrasound-driven microbubbles, Proc. R. Soc. A Math. Phys. Eng. Sci. 464 (2008) 1781–1800, https://doi.org/10.1098/rspa.2007.0362.
[32] K.A. Riske, R. Dimova, Electro-deformation and poration of giant vesicles viewed with high temporal resolution, Biophys. J. 88 (2005) 1143–1155, https://doi.org/10.1529/biophysj.104.050310.
[33] T. Portet, F. Camps I Febrer, J.M. Escoffre, C. Favard, M.P. Rols, D.S. Dean, Visualization of membrane loss during the shrinkage of giant vesicles under electropulsation, Biophys. J. 96 (2009) 4109–4121. doi:10.1016/j.bpj.2009.02.063.
[34] W. Ding, M. Palaiokostas, G. Shahane, W. Wang, M. Orsi, Effects of High Pressure on Phospholipid Bilayers, J. Phys. Chem. B 121 (2017) 9597–9606, https://doi.org/10.1021/acs.jpcb.7b07119.
[35] Y.R. Sliozberg, Structural Changes in Lipid Vesicles Generated by the Shock Blast Waves : Coarse-Grained Molecular Dynamics, Simulation (2013).
[36] K. Inque, T. Kitagawa, Effect of lipid composition on sensitivity of lipid membranes to triton X-100, Biochim. Biophys. Acta - Biomembr. 426 (1976) 1–16, https://doi.org/10.1016/0005-2736(76)90424-7.
[37] B.R. Casadei, C.C. Domingues, E. De Paula, K.A. Riske, Direct visualization of the action of triton X-100 on giant vesicles of erythrocyte membrane lipids, Biophys. J. 106 (2014) 2417–2425, https://doi.org/10.1016/j.bpj.2014.04.039.
[38] J.-P. Franc, J.-M. Michel, Fundamentals of Cavitation, Kluwer Academic Publishers, Dordrecht (2005), https://doi.org/10.1007/1-4020-2233-6.
[39] K.S. Suslick, N.C. Eddingsaas, D.J. Flannigan, S.D. Hopkins, H. Xu, Extreme conditions during multibubble cavitation: sonoluminescence as a spectroscopic probe, Ultrason. Sonochem. 18 (2011) 842–846, https://doi.org/10.1016/j.ultsonch.2010.12.012.
[40] G.L. Chahine, C.-T. Hsiao, Modelling cavitation erosion using fluid–material interaction simulations, Interface Focus 5 (2015) 20150016, https://doi.org/10.1098/rsfs.2015.0016.
[41] C.E. Brennen, Cavitation and bubble dynamics, Oxford University Press, Oxford, 1995.
[42] S. Koda, T. Kimura, T. Kondo, H. Mitome, A standard method to calibrate sonochemical efficiency of an individual reaction system, Ultrason. Sonochem. 10 (2003) 149–156, https://doi.org/10.1016/S1350-4177(03)00084-1.
[43] X. Sun, J.J. Park, H.S. Kim, S. jin S. Lee, A.S. Om, J.Y. Yoon, Experimental Investigation of the Thermal and Disinfection Performances of aNovel Hydrodynamic Cavitation Reactor, Ultrason. Sonochem. 49 (2018) 13–23. doi:10.1016/j.expthermflusci.2018.02.034.
[44] L.M. Cerecedo, C. Dopazo, R. Gomez-Lus, Water disinfection by hydrodynamic cavitation in a rotor-stator device, Ultrason. Sonochem. 48 (2018) 71–78, https://doi.org/10.1016/j.ultsonch.2018.05.015.
[45] J.G. Dalfré Filho, M.P. Assis, A.I.B. Genovez, Bacterial inactivation in artificially and naturally contaminated water using a cavitating jet apparatus, J. Hydro-Environment Res. (2015) 259–267, https://doi.org/10.1016/j.jher.2015.03.001.
[46] L. Albanese, R. Ciriminna, F. Meneguzzo, M. Pagliaro, Energy efficient inactivation of saccharomyces cerevisiae via controlled hydrodynamic cavitation, Energy Sci. Eng. 3 (2015) 221–238, https://doi.org/10.1002/ese3.62.
[47] A. Šarc, J. Kosel, D. Stopar, M. Oder, M. Dular, Removal of bacteria Legionella pneumophila, Escherichia coli, and Bacillus subtilis by (super)cavitation, Ultrason. Sonochem. 42 (2018) 228–236, https://doi.org/10.1016/j.ultsonch.2017.11.004.
[48] M. Zupanc, Ž. Pandur, T. Stepišnik Perdih, D. Stopar, M. Petkovšek, M. Dular, Effects of cavitation on different microorganisms: the current understanding of the mechanisms taking place behind the phenomenon. A review and proposals for further research, Ultrason Sonochem. 57 (2019) 147–165, https://doi.org/10.1016/j.ultsonch.2019.05.009.
[49] B. Balasundaram, S.T.L. Harrison, Study of physical and biological factors involved in the disruption of E. coli by Hydrodynamic Cavitation, Biotechnol. Prog. 22 (2006) 907–913, https://doi.org/10.1021/bp0502173.
[50] B. Balasundaram, S.T.L. Harrison, Optimising orifice geometry for selective release of periplasmic products during cell disruption by hydrodynamic cavitation, Biochem. Eng. J. 54 (2011) 207–209, https://doi.org/10.1016/j.bej.2011.03.002.
[51] S.J. Attwood, Y. Choi, Z. Leonenko, Preparation of DOPC and DPPC supported planar lipid bilayers for atomic force microscopy and atomic force spectroscopy, Int. J. Mol. Sci. 14 (2013) 3514–3539, https://doi.org/10.3390/ijms14023514.
[52] P.R. Adhyapak, S.V. Panchal, A.V.R. Murthy, Cholesterol induced asymmetry in DOPC bilayers probed by AFM force spectroscopy, Biochim. Biophys. Acta - Biomembr. 2018 (1860) 953–959, https://doi.org/10.1016/j.bbamem.2018.01.021.
[53] X. Chen, S. Liu, B. Deme, V. Cristiglio, D. Marquardt, R. Weller, P. Rao, Y. Wang, J. Bradshaw, Efficient internalization of TAT peptide in zwitterionic DOPC phospholipid membrane revealed by neutron diffraction, Biochim. Biophys. Acta - Biomembr. 2017 (1859) 910–916, https://doi.org/10.1016/j.bbamem.2017.01.036.
[54] I.O.L. Bacellar, M.S. Baptista, H.C. Junqueira, M. Wainwright, F. Thalmann, C.M. Marques, A.P. Schroder, Permeability of DOPC bilayers under photoinduced oxidation: Sensitivity to photosensitizer, Biochim. Biophys. Acta - Biomembr. 2018 (1860) 2366–2373, https://doi.org/10.1016/j.bbamem.2018.06.001.
[55] K.J. Fritzsching, J. Kim, G.P. Holland, Probing lipid-cholesterol interactions in DOPC/eSM/Chol and DOPC/DPPC/Chol model lipid rafts with DSC and 13C solid-state NMR, Biochim. Biophys. Acta - Biomembr. 2013 (1828) 1889–1898, https://doi.org/10.1016/j.bbamem.2013.03.028.
[56] P.J. Costa, I. Marques, V. Félix, Interaction of a calix[4]arene derivative with a DOPC bilayer: biomolecular simulations towards chloride transport, Biochim. Biophys. Acta - Biomembr. 2014 (1838) 890–901, https://doi.org/10.1016/j.bbamem.2013.11.021.
[57] A. Moscho, O. Orwar, D.T. Chiu, B.P. Modi, R.N. Zare, Rapid preparation of giant unilamellar vesicles, Proc. Natl. Acad. Sci. 93 (1996) 11443–11447, https://doi.org/10.1073/pnas.93.21.11443.
[58] A. Šarc, T. Stepišnik-Perdih, M. Petkovšek, M. Dular, The issue of cavitation number value in studies of water treatment by hydrodynamic cavitation, Ultrason. Sonochem. 34 (2017) 51–59, https://doi.org/10.1016/j.ultsonch.2016.05.020.
[59] T.J. Mason, Ultrasonic cleaning: An historical perspective, Ultrason. Sonochem. 29 (2016) 519–523, https://doi.org/10.1016/j.ultsonch.2015.05.004.
[60] R.M. Cornell, U. Schwertmann, The Iron Oxides, Wiley-VCH Verlag GmbH & Co. KGaA, Weinheim, FRG, 2003. doi:10.1002/3527602097.
[61] H. Sugita, I. Matsunaga, N. Yanagisawa, H. Tao, Y. Tsutomu, K. Aoki, Effects of pH and Dissolved Ions on Fluorescence Intensity of Sodium Fluorescein, 2003. doi:10.11367/grsj1979.25.211.
[62] Y. Zhou, R.M. Raphael, Solution pH alters mechanical and electrical properties of phosphatidylcholine membranes: Relation between interfacial electrostatics, intramembrane potential, and bending elasticity, Biophys. J. 92 (2007) 2451–2462, https://doi.org/10.1529/biophysj.106.096362.
[63] K.H. de Haas, C. Blom, D. van den Ende, M.H.G. Duits, B. Haveman, J. Mellema, Rheological Behavior of a Dispersion of Small Lipid Bilayer Vesicles, Langmuir 13 (1997) 6658–6668, https://doi.org/10.1021/la970564p.
[64] A. Pal, D.V. Khakhar, Breakage of vesicles in a simple shear flow, Soft Matter. 15 (2019) 1979–1987, https://doi.org/10.1039/c8sm01501e.
[65] E. Saalman, B. Nordén, L. Arvidsson, Y. Hamnerius, P. Höjevik, K.E. Connell, T. Kurucsev, Effect of 2.45 GHz microwave radiation on permeability of unilamellar liposomes to 5(6)-carboxyfluorescein. Evidence of non-thermal leakage, Biochim. Biophys. Acta - Biomembr. 1064 (1991) 124–130, https://doi.org/10.1016/0005-2736(91)90418-8.
[66] A.R. Orlando, G. Mossa, G. D'lnzeo, Effect of microwave radiation on the permeability of carbonic anhydrase loaded unilamellar liposomes, Bioelectromagnetics. 15 (1994) 303–313. doi:doi:10.1002/bem.2250150405.
[67] J. Katz, F. Reuter, H. Sagar, B. el Moctar, R. Mettin, Wall Shear Rates Induced by a Single Cavitation Bubble Collapse, in: Proc. 10th Int. Symp. Cavitation. (2019). doi:10.1115/1.861851_ch208.
[68] L. Cwiklik, P. Jungwirth, Massive oxidation of phospholipid membranes leads to pore creation and bilayer disintegration, Chem. Phys. Lett. 486 (2010) 99–103, https://doi.org/10.1016/j.cplett.2010.01.010.
[69] A. Schroeder, J. Kost, Y. Barenholz, Ultrasound, liposomes, and drug delivery: principles for using ultrasound to control the release of drugs from liposomes, Chem. Phys. Lipids. 162 (2009) 1–16, https://doi.org/10.1016/j.chemphyslip.2009.08.003.
[70] M. Pong, S. Umchid, A.J. Guarino, P.A. Lewin, J. Litniewski, A. Nowicki, S.P. Wrenn, In vitro ultrasound-mediated leakage from phospholipid vesicles, Ultrasonics. 45 (2006) 133–145, https://doi.org/10.1016/j.ultras.2006.07.021.
[71] D.L. Miller, S.V. Pislaru, J.F. Greenleaf, Sonoporation: Mechanical DNA delivery by ultrasonic cavitation, Somat. Cell Mol. Genet. 27 (2002) 115–134, https://doi.org/10.1023/A:1022983907223.
[72] H.Y. Lin, J.L. Thomas, Factors affecting responsivity of unilamellar liposomes to 20 kHz ultrasound, Langmuir 20 (2004) 6100–6106, https://doi.org/10.1021/la049866z.
[73] A. Schroeder, Y. Avnir, S. Weisman, Y. Najajreh, A. Gabizon, Y. Talmon, J. Kost, Y. Barenholz, Controlling liposomal drug release with low frequency ultrasound: Mechanism and feasibility, Langmuir 23 (2007) 4019–4025, https://doi.org/10.1021/la0631668.
[74] E.F. Small, N.R. Dan, S.P. Wrenn, Low-frequency ultrasound-induced transport across non-raft-forming ternary lipid bilayers, Langmuir 28 (2012) 14364–14372, https://doi.org/10.1021/la303183b.
[75] T. Yamaguchi, M. Nomura, T. Matsuoka, S. Koda, Effects of frequency and power of ultrasound on the size reduction of liposome, Chem. Phys. Lipids 160 (2009) 58–62, https://doi.org/10.1016/j.chemphyslip.2009.04.002.
[76] L. Saunders, J. Perrin, D. Gammack, Ultrasonic irradiation of some phospholipid sols, J. Pharm. Pharmacol. 14 (1962) 567–572, https://doi.org/10.1111/j.2042-7158.1962.tb11141.x.

[77] A. Ferrari, Fluid dynamics of acoustic and hydrodynamic cavitation in hydraulic power systems, Proc. R. Soc. A Math. Phys Eng. Sci. 473 (2017), https://doi.org/10.1098/rspa.2016.0345.
[78] V.S. Moholkar, P. Senthil Kumar, A.B. Pandit, Hydrodynamic cavitation for sonochemical effects, Ultrason, Sonochem. 6 (1999) 53–65, https://doi.org/10.1016/S1350-4177(98)00030-3.
[79] J. Park, J. Church, Y. Son, K.T. Kim, W.H. Lee, Recent advances in ultrasonic treatment: Challenges and field applications for controlling harmful algal blooms (HABs), Ultrason. Sonochem. 38 (2017) 326–334, https://doi.org/10.1016/j.ultsonch.2017.03.003.
[80] J. Wang, Z. Wang, C.L.Z. Vieira, J.M. Wolfson, G. Pingtian, S. Huang, Review on the treatment of organic pollutants in water by ultrasonic technology, Ultrason. Sonochem. (2019), https://doi.org/10.1016/j.ultsonch.2019.01.017.
[81] Y.L. Chen, H.H. Chang, Y.C. Chiang, C.P. Lin, Application and development of ultrasonics in dentistry, J. Formos. Med. Assoc. 112 (2013) 659–665, https://doi.org/10.1016/j.jfma.2013.05.007.
[82] P.R. Gogate, A.M. Kabadi, A review of applications of cavitation in biochemical engineering/biotechnology, Biochem. Eng. J. 44 (2009) 60–72, https://doi.org/10.1016/j.bej.2008.10.006.
[83] No Title, (n.d.). doi:10.1111/jfpe.13144.
[84] C.R. Holkar, A.J. Jadhav, D.V. Pinjari, A.B. Pandit, Cavitationally Driven Transformations: A Technique of Process Intensification, Ind. Eng. Chem. Res. 58 (2019) 5797–5819, https://doi.org/10.1021/acs.iecr.8b04524.